Influence of H_{c1} on the irreversibility line in $YBa_2Cu_3O_7$ thin films

L. Civale, T. K. Worthington, and A. Gupta
IBM Thomas J. Watson Research Center, Yorktown Heights, New York 10598-0213
(Received 17 August 1992; revised manuscript received 2 February 1993)

The irreversibility line of a type-II superconductor separates the H-T plane into a region above the line where the critical current is zero and the magnetic properties are reversible, and a region below where a critical current is observed and the magnetic properties are irreversible. Although there is great controversy over the various models proposed to explain these observations, they all depend on the existence of magnetic-flux quanta in the sample. This implies that the irreversibility line cannot cross $H_{c1}(T)$. In bulk samples, assuming that the observed functional forms are maintained, this would be expected to occur much too close to T_c to be observed. However, for films thinner than the London penetration depth, when the field is applied parallel to the film surface, H_{c1} can be greatly enhanced. We report the results of measurements of the irreversibility line in thin $YBa_2Cu_3O_7$ films that clearly show deviation from the power-law behavior observed for bulk samples. This deviation is in good agreement with calculations of the enhanced H_{c1}, which can be as large as several tesla for films thinner than ~ 250 Å.

I. INTRODUCTION

It is now well established that high-T_c superconductors have a magnetic phase diagram that is more complex than in the case of the traditional type-II superconductors. In addition to the lower critical field H_{c1} and the upper critical field H_{c2}, these superconductors exhibit a third characteristic line located between the two critical fields in the H-T plane. This *irreversibility line* $H_{\rm irr}(T)$ first observed by Müller *et al.*[1] in polycrystalline La_2CuO_{4-y}:Ba was originally defined as the boundary between a reversible regime having zero critical current density J_c and an irreversible or hysteretic regime with finite J_c.

The vortex dynamics in the vicinity of the irreversibility line were subsequently explored using a variety of magnetic and transport (both ac and dc) techniques. However, considerable controversy remains as to whether this line represents a true phase transition, as is asserted by the vortex-lattice melting[2–4] and vortex-glass theories[5,6] or a dynamic crossover, as in the giant flux-creep description.[7–9] However, all of the models assume the existence of magnetic-flux vortices. This implies that, irrespective of the model, the irreversibility line cannot cross $H_{c1}(T)$ since below this line at equilibrium there are no vortices present in the sample. For bulk $YBa_2Cu_3O_7$ samples, the irreversibility line is observed to have a temperature dependence given by $H_{\rm irr}(T) \propto (1-T/T_c)^{\alpha}$. Reported values for the exponent α obtained by a variety of techniques, range between 4/3 and 2.[1,7,10–12] The lower critical field H_{c1}, on the other hand, has a linear temperature dependence near T_c, in agreement with Ginzburg-Landau theory.[13] These two different temperature dependencies imply that the simple power-law behavior of $H_{\rm irr}(T)$ must break down since it cannot cross $H_{c1}(T)$. Assuming that both functional forms are maintained arbitrarily close to T_c, for bulk $YBa_2Cu_3O_7$ the intersection between $H_{c1}(T)$ and $H_{\rm irr}(T)$ occurs at $(T_c - T) < 10^{-7}$ K, and is therefore experimentally inaccessible. However, for a film with thickness τ, less than the London penetration depth λ, when the applied field is parallel to the surface of a film, H_{c1} is enhanced[14] and, as we will show in this paper, this produces a significant effect on the location of $H_{\rm irr}(T)$.

II. EXPERIMENTAL TECHNIQUE

This work extends our previous study on the thickness dependence of $H_{\rm irr}(T)$, in which only the $H \| c$ orientation was considered,[15] and the same films were used. The irreversibility line was measured using the same ac technique. A small copper coil was placed on the surface of the film. The inductance L and series resistance R of the coil were measured as the temperature was slowly decreased. The 1 MHz measuring current in the coil produces an ac magnetic field with a spatial distribution similar to that of a magnetic dipole perpendicular to the film surface and induces ac currents lying in the Cu-O planes of the film. The amplitude of the ac field on the surface of the film was $h_{\rm ac} \sim 0.05$ Oe at the axis of the coil. A uniform dc field H of up to 9 T was provided by a superconducting magnet in persistent mode. The dc field was carefully aligned parallel to the film surface to better than 1°. This alignment was confirmed by deliberate misalignment of $\pm 1°$, 2°, and 5°. The temperature resolution is ~ 20 mK.

The connection between the ac susceptibility and the irreversibility line is a nontrivial and controversial issue and we will discuss it to a certain extent. The original and most intuitive definition of the irreversible line, namely the boundary between nonzero and zero J_c regimes, has clear difficulties which originate in the vagueness of the definition of critical current in the presence of large thermal relaxation. A better definition is the determination of the onset of nonlinear behavior in the I-V

curves. The nonlinearity of an I-V isotherm in the mixed state is a clear indication of the existence of flux pinning at that temperature and field, even if that pinning is not strong enough to sustain measurable persistent currents. This is the definition that we will adopt here.

In our ac susceptibility technique, the changes in L and R reflect variation of the real and imaginary parts of the susceptibility of the film χ' and χ'', respectively. The variations in both components are determined by the induced currents flowing in the film, χ' measures the screening produced by those currents, and χ'' measures the dissipation. Therefore they contain information on the linear or nonlinear character of the I-V curves. As the film is cooled, a step in χ' and a coincident peak in χ'' are observed. We have used the location of the maximum in χ'' as an *estimation* of $T_{\rm irr}(H)$. The simplistic association of the peak in χ'' with the irreversibility line has been correctly criticized in the past.[16,17] The peak in χ'' can occur above T_c or far into the nonlinear I-V region well below the irreversibility line depending on the experimental parameters.[16,18] However, we will argue below that for these films and our experimental parameters, the peak occurs *below* the irreversibility line.

The induced currents decay as a function of the depth from the surface. Aside from geometry-dependent numerical factors of order 1, the maximum in χ'' (which roughly coincides with half screening as measured by χ') occurs when the screening currents flow in a depth equal to the size of the sample. In a normal metal, the length scale for the decay of the screening currents is the skin depth $\delta_n=(c/2\pi)\sqrt{\rho_n/f}$, where ρ_n is the normal-state resistivity and f is the frequency. An analogous situation occurs in a pinning free type-II superconductor, where $\delta_{\rm ff}=(c/2\pi)\sqrt{\rho_{\rm ff}/f}$, is the flux-flow skin depth at the flux-flow resistivity $\rho_{\rm ff}$. In this case, due to the strong temperature and field dependence of $\delta_{\rm ff}$, a peak in χ'' can be observed when T is varied at constant H (or vice versa).[19,20] In both cases the behavior is ohmic, in the sense that ρ_n and $\rho_{\rm ff}$ are independent of the current density, i.e., the I-V curves are linear. As a consequence, the ac response is *linear,* i.e., χ is independent of the amplitude of the ac field $h_{\rm ac}$ and there is no harmonic generation. On the other hand, χ will be frequency dependent[19] through $\delta_{\rm ff}(\omega)$. When pinning becomes relevant, the I-V curves of the superconductor become nonlinear.[21] Be defining a nonlinear resistivity, an amplitude-dependent δ can be estimated.[16] In this case the ac susceptibility is nonlinear, i.e., χ' and χ'' is fixed T and H depend on $h_{\rm ac}$, and harmonic generation occurs.[17] In a previous work[18] we have shown that both behaviors can be experimentally observed in the same $YBa_2Cu_3O_7$ single crystal by varying the frequency of the ac field. The relevant sample dimension in our experimental configuration is the sample thickness τ. At high enough frequency the condition $\delta_{\rm ff}\simeq\tau$ occurs at ρ values large enough to be in the flux-flow reversible regime. By reducing the frequency, that condition can be shifted to smaller ρ values (thus shifting the peak in χ'' to lower T), until the nonlinear pinning dominated regime is accessed. We have also shown[18] that at low enough frequency the amplitude dependence of χ' is well described by the critical-state model,[22] and that J_c values can be extracted from those data. In this case it is convenient to define an amplitude-dependent critical-state penetration distance $L_p=(c/4\pi)h_{\rm ac}/J_c$, which describes the length over which the supercurrent flows in order to screen the interior of the sample from the ac field.[20]

In a real sample the change from linear flux-flow behavior to nonlinear superconducting behavior can make analysis of the ac susceptibility very complicated. However, for our films and our experimental conditions, the maximum in χ'' always occurs in the pinning dominated regime. We present results on two films of thickness 6000 and 250 Å. An applied ac field $h_{\rm as}=0.05$ Oe induces a current density of $\sim 10^2$–10^4 A/cm^2 at half screening in the thicker and thinner film respectively. At $f=1$ MHz, the condition $\delta_{\rm ff}\simeq\tau$ would occur at $\rho\sim 1.4\times10^{-4}$ and $2.5\times10^{-7}\mu\Omega$ cm respectively. These values are orders of magnitude smaller than the resistivity levels where nonlinear behavior starts to develop in the I-V curves of $Yba_2Cu_3O_7$ films,[23] thus indicating that the peak in χ'' develops deep into the nonlinear, pinning dominated regime. This conclusion is confirmed[15] by the strong amplitude dependence of χ'' in these films. Thus for the case of thin films, the line in the H-T plane defined by the maximum in χ'', measured at 1 MHz with an ac field of 0.05 Oe represents a lower bound for the location of the irreversibility line.

It is important to remember that the I-V curves in the pinning dominated regime become linear (again) at a lower current density. This occurs either through the movement of vortices in the thermally assisted flux-flow (TAFF) regime[24,25] or when the vortices remain trapped and oscillate inside their pining wells, in which case the responses of the sample is determined by the Campbell penetration depth.[26] The complicated ac response of the vortex system when all of these phenomena are taken into account has been recently explored in detail by Clem and Coffey.[20] However, in our ac technique, when the temperature is lowered from above T_c, the vortex system will necessarily cross a nonlinear portion of the I-V curves before entering into either the TAFF or Campbell regime, and thus an amplitude dependence will be observed. On the contrary, if the peak in χ'' occurs in the flux-flow regime, which is linear for all current densities, (disregarding, of course, self-heating effects at very high current), there is no amplitude dependence. The previous analysis is thus unaffected by the inclusion of these additional phenomena.

III. RESULTS

Figure 1(a) shows the irreversibility line of the 6000 Å film, both for H parallel and perpendicular to the c axis. Apparent in the figure are both the upward curvature of $H_{\rm irr}$ in both configurations and the anisotropy. Figure 1(b) shows the same data now plotted at H vs $(1-t)$ on a log-log scale, where $t=T/T_c$ is the reduced temperature. It is seen that both data sets follow a straight line over the entire field range, which implies a power-law relation, $H_{\rm irr}=C(1-t)^{\alpha}$. The critical temperature used to generate this figure is the temperature of the maximum in χ''

at zero field; it is not an adjustable parameter. The value for this film is $T_c = 90.1$ K. The solid lines represent least-squares fits to a power law. The fitting parameters are $C_{\parallel} = 81$ T and $\alpha_{\parallel} = 1.21$ for the $H \| c$ case, and $C_{\perp} = 398$ T and $\alpha_{\perp} = 1.22$ in the $H \perp c$ case. The exponents are similar although a bit smaller than those usually observed in $YBa_2Cu_3O_7$ single crystals.[10] Due to the similarity between $\alpha_{\parallel}$ and $\alpha_{\perp}$, the anisotropy is essentially field independent, and its value $C_{\perp}/C_{\parallel} \simeq 4.9$ is similar to that reported for H_{c2} in crystals.[27] The similarity between the data of Fig. 1 and those of single crystals[10] indicate that H_{irr} in this sample, in both configurations, is determined by bulk properties and not by size effects.

In order to observe a significant size effect in H_{irr}, a much thinner film must be measured. Figures 2(a) and 2(b) are the equivalent of Figs. 1(a) and 1(b) for a film 250 Å thick. Comparison of Figs. 1(a) and 2(a) reveals interesting differences in both field configurations. In the $H \| c$ case, H_{irr} of the thinner film is shifted to lower temperatures with respect to the thicker one. This effect was discussed in our previous work.[15] For the $H \perp c$ case, a new feature is apparent in the thinner film, namely the existence of a region of opposite curvature in H_{irr} at low fields. At higher fields ($H > 3$ T), H_{irr} in this configuration is similar to that of the 6000 Å film.

The log-log plot of Fig. 2(b) provides further insight. For $H \| c$, a good agreement with a single power law is found in the whole experimental range; the best-fit parameters are $C_{\parallel} = 103$ T and $\alpha_{\parallel} = 1.54$. In the $H \perp c$ case, the power law holds only at high field. A least-squares fit to the data for $H > 3$ T yields $C_{\perp} = 331$ T and $\alpha_{\perp} = 1.17$. The breakdown of the power law in the low-field region is clearly observed as a departure of the experimental data from the straight line representing the extrapolation of the high-field data show in Fig. 2(b). We emphasize again that T_c is taken as the position of the maximum in χ'' at $H = 0$. The value for this sample is $T_c = 89.07$ K.

The fact that this anomaly is only observed in very thin films, and only when the applied field is parallel to the film surface, suggests that its origin is a size effect. The thickness of the film, 250 Å, is still large compared to the superconducting coherence length ξ except for a temperature range of a few millidegrees below T_c, and so the possibility that the observed phenomenon is related to a size effect on the upper critical field H_{c2} can be ruled out. However, the film thickness is smaller than the London penetration depth λ and therefore the magnetic-field distribution within the film, both in the Meissner and mixed

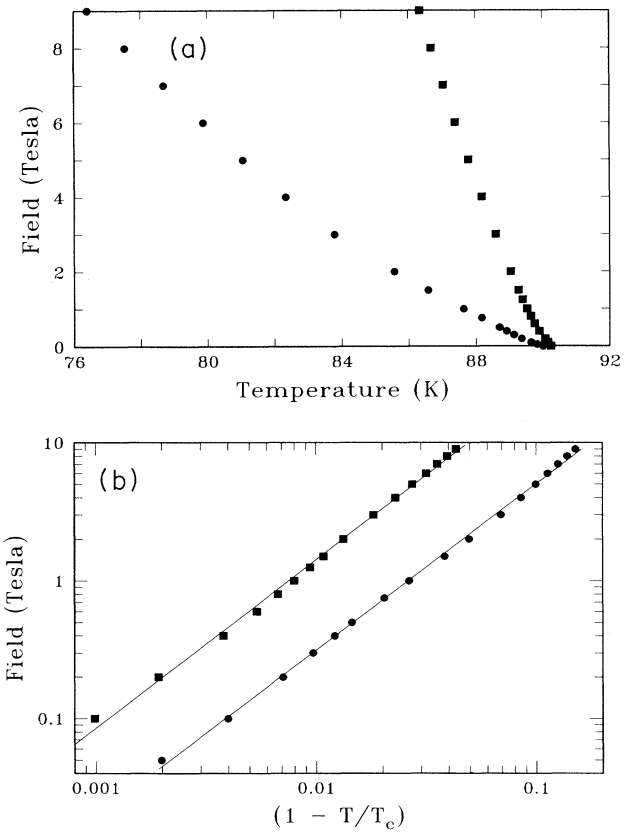

FIG. 1. (a) The irreversibility line of a 6000 Å film, defined by the maximum in χ'' for fields parallel (○) and perpendicular (□) to the c axis. (b) shows the same data plotted as a function of $(1-t)$.

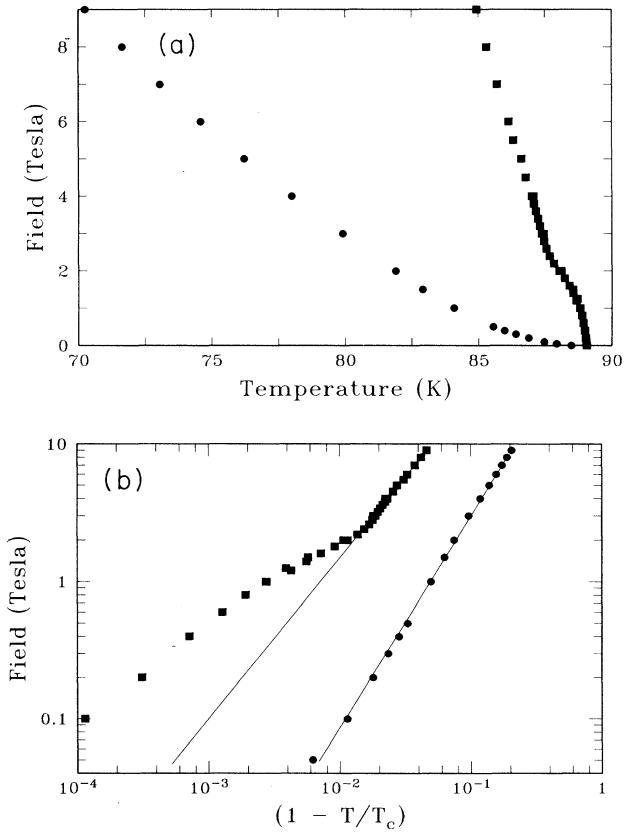

FIG. 2. (a) The irreversibility line of a 250 Å film, defined by the maximum in χ'' for fields parallel (○) and perpendicular (□) to the c axis. (b) shows the same data plotted as a function of $(1-t)$.

states, is very different from that in a bulk sample which results in an enhancement of H_{c1}.

IV. THEORY AND DISCUSSION

The lower critical field H_{c1}^{τ} of a slab of thickness τ when the applied field is parallel to the sample surface was first calculated by Abrikosov.[14,28] In the London approximation, where the energy of the core can be neglected,

$$H_{c1}^{\tau}=H_{c1}^{\infty}\frac{1+\frac{2}{K_0(1/\kappa)}\sum_{n=1}^{\infty}(-1)^n K_0(n\tau/\lambda)}{1-\cosh^{-1}(\tau/2\lambda)}\ , \qquad (1)$$

where H_{c1}^{∞} is the lower critical field of an infinite sample of the same material, $\kappa=\lambda/\xi$ is the Ginzburg-Landau parameter, and K_0 is the Hankel function of zero order and imaginary argument. In the appendix we will present a different and we hope, a more intuitive derivation for this expression, which can be generalized to geometries other than slabs. Equation (1) implies that H_{c1} of a thin sample in $H\|$ surface configuration will be always larger than in the bulk material. The most important contribution to that enhancement is the denominator of (1), which tends to zero when $\tau\ll\lambda$. Physically, this factor reflects the fact that when the sample is thinner than the penetration depth, the internal field in the Meissner state is only slightly lower than the applied field. As a consequence, the energy cost of this partial field expulsion is smaller, and the nucleation of a vortex is not favorable until H reaches a larger value. The physical meaning of the sum of Hankel functions is described in detail in the Appendix.

In the limit of $\tau\ll\lambda$, Eq. (1) can be approximated as follows. First, $[1-\cosh^{-1}(\tau/2\lambda)]\simeq(\tau/2\lambda)^2/2$. Second, the series of K_0 functions can be split in positive and negative terms; each subseries can then be approximated by an integral and the results then subtracted, giving

$$\sum_{n=1}^{\infty}(-1)^n K_0(n\tau/\lambda)\simeq\frac{1}{2}\ln(\tau/\lambda)-0.289\ .$$

With these approximations, Eq. (1) becomes

$$H_{c1}^{\tau}\simeq\frac{2\Phi_0}{\pi\tau^2}[\ln(\tau/\xi)-0.458],\quad(\tau\ll\lambda)\ . \qquad (2)$$

This expression is similar to the usual results for H_{c1} in an infinite sample, except that the temperature-dependent length λ is replaced by τ and the only remaining temperature dependence is in the logarithmic term. In this limit H_{c1}^{τ} is independent of λ.

These results are valid for an isotropic superconductor. For the case of anisotropic superconductors, the calculation has be extended using the anisotropic London approximation.[29] The results are expressions identical to Eqs. (1) and (2) with the appropriate bulk anisotropic parameters, which in this case are $H_{c1\|ab}$, κ_{ab}, and λ_{ab} (see the Appendix).

We can compare the prediction of Eq. (1) with our measurement of the irreversibility line using bulk values for $\lambda=1300$ Å (Ref. 12), and $\kappa=300$, (Ref. 23), $H_{c1}^{\infty}=180$ Oe, (Ref. 12), and assuming the G-L temperature dependencies for λ and H_{c1}^{∞}. We have plotted the calculated value of $H_{c1}^{\tau}(T)$ (solid line), along with our data for the irreversibility line in Fig. 3. It is important to keep in mind that our data are still an estimation of the irreversibility line. We are not measuring H_{c1}, but are only showing that the irreversibility line is shifted up as a consequence of the large H_{c1} in this configuration. This effect is convincingly seen in Fig. 3, particularly considering that there are *no adjustable parameters* in the calculation of H_{c1}^{τ}.

As we have pointed out before, for these samples and experimental conditions, the peak in χ'' is a lower bound to the location of the irreversibility line. By reducing the frequency, the peak will shift to a lower temperature, but as we have already underestimated the irreversibility temperature, this will only result in a worse estimation.

The value of H_{c1}^{τ} is extremely sensitive to the thickness, τ which is also the least well-known parameter in this calculation. It is deduced from the thickness of thicker films measured with a Dek-Tak and the number of laser ablation pulses. It is estimated that the calculated thickness is accurate to ±50 Å. If we vary the thickness in our comparison we can get a better agreement between the measured values of the irreversibility line and the calculated value of H_{c1}. The dotted line in Fig. 3 is for a film thickness of 210 Å, a value well within the error estimates. We have seen this enhancement in the irreversibility line in several films thinner than 1500 Å.

The above calculation of H_{c1}^{τ} fails when the film thickness approaches the superconducting coherence length ξ. This can be easily verified in the approximate expression (2), which gives a negative H_{c1}^{τ} for $\tau<1.58\xi$. This is not surprising, since in that limit the core of the vortex will be of the size of the sample and the London approxima-

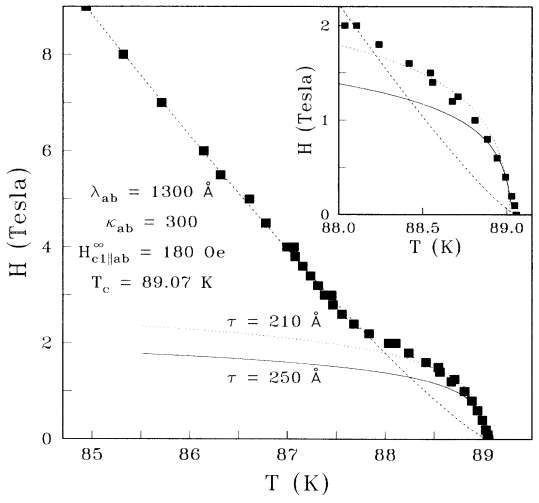

FIG. 3. The irreversibility line of the 250 Å film for fields parallel to the *ab* plane. The dashed line is the power-law behavior of the high-field data extrapolated to low field. The solid and dotted lines are calculated values of $H_{c1}^{\tau}(T)$ from Eq. (1) for film thickness of 250 and 210 Å, respectively.

tion will not be valid. It is known that for $\tau < 1.81\xi$, the energetically most favorable solution of the G-L equations corresponds to a uniform superconducting order parameter throughout the sample[30] i.e., in this limit there will *never* be any vortices in the film. For our film this condition occurs when $1.81\xi_{ab}(0)/\sqrt{1-t} > 250$ Å, which is satisfied for $(T_c - T) < 0.06$ K, a temperature window only slightly larger than our experimental resolution. In our thinnest film of nominal 100 Å thickness, there is evidence of a different behavior in a region of $\simeq 0.4$ K below T_c, consistent with a size effect due to the coherence length becoming of the order of the film thickness.

The equilibrium array of vortices in absence of pinning in thin films with H parallel to the surface differs from the Abrikosov lattice in bulk superconductors.[31] Due to the repulsion from the surface, there is a range of fields above H_{c1}^{τ} in which the flux lines lie in one row along the center plane. The vortex spacing in that regime (which is different than the Abrikosov lattice constant in bulk samples at the same field), and the field where the vortex system switches from one line of vortices to a staggered array can be numerically calculated.[31] The presence of a dense distribution of pinning sites destroys the perfect order but it has little effect in the dimensional crossover. In our 250 Å film, the dimensional crossover field exceeds our maximum available field of 9 T; in spite of this the location of $H_{\rm irr}$ for $H \perp c$ is almost identical to that in the 6000 Å film, where the dimensional crossover occurs below 0.1 T. This indicates that our experimental technique is probing the dynamics of individual flux lines oscillating with amplitude much smaller than the intervortex spacing.

In conclusion, we have measured the irreversibility line of thin films for the case of an applied field parallel to the film surface. When the film is thinner than the penetration depth, the size effect on H_{c1} can be very large. We have calculated the enhancement of H_{c1} using a simple image technique, and shown that the observed anomalies in $H_{\rm irr}(T)$ near T_c are consistent with this calculation for a film of nominal 250 Å thickness.

ACKNOWLEDGMENTS

We gratefully acknowledge valuable discussions with P. M. Marcus.

APPENDIX

The lower critical field of a superconducting sample is defined as the field where the nucleation of the first vortex in the sample becomes energetically favorable. This occurs when the Gibbs free energy of the sample with no vortices is the same as with just one vortex inside it. We assume that our sample is infinite in the z direction, and has uniform cross section. We will also assume that the applied field H is uniform and parallel to z. In this geometry all the quantities involved in the problem will be independent of z. The magnetic field $\mathbf{h}(\mathbf{r})$ [where $\mathbf{r}=(x,y)$] will be parallel to z everywhere, and the supercurrents will flow in the x-y plane. If we restrict our analysis to the limit of $\kappa \gg 1$, the London limit, the core energy of the vortex nucleated in the sample can be neglected, and the Gibbs free energy per unit length G along z, is given by[32]

$$G = F + \frac{1}{8\pi}\int_S (h^2 + \lambda^2 |\nabla + \mathbf{h}|^2) dS - \frac{H}{4\pi}\int_S h\, dS \ , \quad \text{(A1)}$$

where F is the Helmholtz free energy per unit length. The integrals extend over the cross section of the sample S which so far is assumed to have an arbitrary shape. We will later constrain S to the particular case of a slab. The first integral accounts for the magnetic energy (h^2) and the kinetic energy of the supercurrents ($\lambda^2 |\nabla \times \mathbf{h}|^2$). The second integral can be thought as the contribution of a "magnetic pressure." When H_{c1} is calculated for an infinite sample, the magnetic field in absence of a vortex is zero, and Eq. (A1) in the Meissner state reduces to $G = F$. In a finite sample, however, the internal field in the Meissner state $h_M(\mathbf{r})$ is nonzero, and must be calculated using the London equation

$$h_M - \lambda^2 \nabla^2 h_M = 0 \ , \quad \text{(A2)}$$

with the boundary condition (BC) $h_M = H$ on the surface. Equation (A2) implies that h_M decays from the surface in a characteristic distance λ. If any of the dimensions of the sample is of the order of λ or smaller, h_M will be non-negligible everywhere. In these conditions the interaction between the surface currents and a vortex located anywhere in the sample are important and H_{c1} will be perturbed.

If there is one vortex located at $\mathbf{r}_0 = (x_0, y_0)$, the field in the sample, $h_1(\mathbf{r})$, can be obtained from

$$h_1 - \lambda^2 \nabla^2 h_1 = \Phi_0 \delta(\mathbf{r}_0) \ , \quad \text{(A3)}$$

again with the BC $h_1 = H$ on the surface. It is convenient to decompose h_1 into the sum of two components, $H_1 = h_M + h_V$, where h_M is the solution of (A2), (with the BC $h_M = H$ on the surface), and $h_V(\mathbf{r})$ is the solution of (A3) with the BC $h_V = 0$ on the surface. The standard procedure[32] to calculate G is to transform (A1) using vector identities into

$$G = F + \frac{1}{8\pi}\int_S (\mathbf{h} - \lambda^2 \nabla^2 \mathbf{h}) \cdot \mathbf{h}\, dS + \frac{\lambda^2}{8\pi}\int_C [\mathbf{h} \times (\nabla \times \mathbf{h})] \cdot \mathbf{n}\, dl - \frac{H}{4\pi}\int_S h\, dS \ , \quad \text{(A4)}$$

where the line integral extends through the contour C of the cross section S and $\mathbf{n}$ is the external normal to that contour. Unlike the case of an infinite superconductor, in a finite sample this line integral does not vanish. We can now calculate $\Delta G = G(h_M + h_V) - G(h_M)$. According to (A2), the first integral of (A4) vanishes when there are no vortices present. When there is a single vortex, according to (A3), this term contributes with $(1/8\pi)\Phi_0 h_1(\mathbf{r}_0)$. The last integral in (A4) is simply the total flux through the sample cross section. The line integral can be split in various terms by decomposing $\mathbf{h}$ into its components h_M and h_V. After some calculation, and using the BC for h_V,

we obtain

$$\Delta G=\frac{\Phi_0}{8\pi}h_1(\mathbf{r}_0)+\frac{\lambda^2}{8\pi}\int_C[h_M\times(\nabla\times h_V)]\cdot\mathbf{n}\,dl - \frac{H}{4\pi}\Phi_V(\mathbf{r}_0)\ . \tag{A5}$$

Here $\Phi_V(\mathbf{r}_0)=\int_S h_V dS$ is the magnetic flux through the sample associated with the vortex located at $\mathbf{r}_0$. Using the Maxwell equation $\nabla\times\mathbf{h}=(4\pi/c)\mathbf{J}$, the BC for h_M and fluxoid quantization, the line integral can be further transformed into

$$\frac{\lambda^2}{8\pi}\int_C[h_M\times(\nabla\times h_V)]\cdot\mathbf{n}\,dl=\frac{H}{8\pi}(\Phi_V(\mathbf{r}_0)-\Phi_0)\ .$$

Replacing in (A5), we obtain finally

$$\Delta G=\frac{\Phi_0}{8\pi}[h_M(\mathbf{r}_0)+h_V(\mathbf{r}_0)]-\frac{H}{8\pi}[\Phi_0+\Phi_V(\mathbf{r}_0)]\ . \tag{A6}$$

The values of $h_M(\mathbf{r}_0)$, $h_V(\mathbf{r}_0)$, and $\Phi_V(\mathbf{r}_0)$ can in principle be calculated for a sample of arbitrary geometry. Noticing that h_M is proportional to H [Eq. (A2)], that h_V is independent of H and its scale is determined by Φ_0/λ^2 [Eq. (A3)], and that Φ_V is a fraction of Φ_0, it is useful to rewrite these functions in the form $h_M(\mathbf{r}_0)=H\mathcal{P}(\mathbf{r}_0)$, $h_V(\mathbf{r}_0)=H_{c1}^{\infty}\mathcal{Q}(\mathbf{r}_0)$, and $\Phi_V(\mathbf{r}_0)=\Phi_0\mathcal{R}(\mathbf{r}_0)$. The dimensionless functions $\mathcal{P}$, $\mathcal{Q}$ and $\mathcal{R}$ depend solely on the sample shape, and are size scaled by λ. The field $H_{\rm nucl}$ at which the nucleation of a vortex becomes energetically favorable is then obtained through the condition $\Delta G=0$:

$$H_{\rm nucl}(\mathbf{r}_0)=H_{c1}^{\tau}\frac{\mathcal{Q}(\mathbf{r}_0)}{1+\mathcal{R}(\mathbf{r}_0)-\mathcal{P}(\mathbf{r}_0)}\ . \tag{A7}$$

Unlike the situation for an infinite sample, that field will be dependent on the position $\mathbf{r}_0$ of the vortex core. For each geometry, there will be a particular choice of $\mathbf{r}_0$ that gives the minimum nucleation field. The first vortex will nucleate at that position, and the corresponding $H_{\rm nucl}$ is the H_{c1} of that sample.

We will now use (A7) to calculate H_{c1} in the particular case of an infinite slab of thickness τ, extending from $x=-\tau/2$ to $x=\tau/2$, and infinite in the y direction. Due to the symmetry, it is clear that the energetically most favorable position for the nucleation of the first vortex is any point on the center line of the slab. The Meissner field at $x=0$ is $h_M=H/\cosh(\tau/2\lambda)$ i.e., $\mathcal{P}=1/\cosh(\tau/2\lambda)$. To calculate h_V we note that the field associated with the vortex is not the same as in an infinite sample, which is given[32] by $h_V^{\infty}=(\Phi_0/2\pi\lambda^2)K_0(r/\lambda)$ for $r>\xi$ and $h_V^{\infty}=(\Phi_0/2\pi\lambda^2)K_0(\xi/\lambda)$ for $r<\xi$. Although h_V^{∞} satisfies (A3), it does not satisfy the BC $h_V=0$ on the surface of the slab. The physical meaning of this problem is that the cylindrically symmetric current distribution associated with h_V^{∞} has a nonzero normal component on the surface. We must add some contribution to h_V to cancel that component. That problem was solved by Bean and Livingston[33] by superimposing the field generated by an image antivortex located outside the sample symmetrically with respect to the real vortex. As the slab has two surfaces, we must add two image antivortices, one at each side of the sample. If the vortex is located at $x=0$, the images will be located at $x=\pm\tau$. But the current distribution associated with each image will in turn introduce a normal component of J on the opposite surface that must be compensated by adding two new images (positive in this case) at a distance 2τ from the center. This procedure must be repeated indefinitely. Each new pair of images, of alternating sign, will introduce a smaller perturbation in the region $-\tau\le x\le\tau$, and the series will converge. The value of h_V at the location of the real vortex is the superposition of the contributions of all these images,

$$h_V(0)=h_V^{\infty}(0)+2\sum_{n=1}^{\infty}(-1)^n h_V^{\infty}(n\tau/\lambda) =H_{c1}^{\infty}\left[2\left[1+\frac{2}{K_0(1/\kappa)}\right]\sum_{n=1}^{\infty}(-1)^n K_0(n\tau/\lambda)\right]\ ,$$

where the relation $H_{c1}=h_V^{\infty}(0)/2$ has been used. (The expression in brackets corresponds to $\mathcal{Q}$).

Finally, the magnetic flux associated with the vortex is given by,[34] $\Phi_V=\Phi_0[1-1/\cosh(\tau/2\lambda)]$, where the factor in brackets is $\mathcal{R}$, which is always smaller than 1. The nonvanishing current at the surface accounts for the difference to satisfy the condition that the associated fluxoid is Φ_0. By replacing all these results in (A7) we obtain Eq. (1).

The previous calculation can be easily generalized for anisotropic superconductors using the anisotropic London approximation.[29] Since in our case the vortex is in the ab plane, the value of H_{c1}^{∞} is the value for $H\|ab$, and κ is κ_{ab}. The supercurrents that determine both the penetration of the external field, and the decay of the field of the vortex and its images in the direction of the film thickness, flow only in the Cu-O planes, so the appropriate λ to compare with τ is λ_{ab}.

[1]K. A. Müller, M. Takashige, and J. G. Bednorz, Phys. Rev. Lett. **58**, 1143 (1987).
[2]P. L. Gammel, L. F. Schneemeyer, J. V. Waszczak, and D. J. Bishop, Phys. Rev. Lett. **61**, 1666 (1988).
[3]D. R. Nelson, Phys. Rev. Lett. **60**, 1973 (1988).
[4]A. Houghton, R. A. Pelcovitz, and A. Sudbo, Phys. Rev. B **40**, 6763 (1989).
[5]M. P. A. Fisher, Phys. Rev. Lett. **62**, 1415 (1989).
[6]D. S. Fisher, M. P. A. Fisher, and D. A. Huse, Phys. Rev. B **43**, 130 (1991).
[7]Y. Yeshurn and A. P. Malozemoff, Phys. Rev. Lett. **60**, 2202 (1988).
[8]A. P. Malozemoff, T. K. Worthington, Y. Yeshurun, F. Holtzberg, and P. Kes, Phys. Rev. B **38**, 7203 (1988).
[9]E. Brandt, Phys. Rev. Lett. **67**, 2219 (1991).
[10]T. K. Worthington, W. J. Gallagher, D. L. Kaiser, F. Holtzberg, and T. R. Dinger, Physica **153 - 155C**, 32 (1987).
[11]D. E. Farrell, J. P. Rice, and D. M. Ginsburg, Phys. Rev. Lett.

67, 1165 (1991).
[12]L. Krusin-Elbaum, L. Civale, F. Holtzberg, A. P. Malozemoff, and C. Feild, Phys. Rev. Lett. **67**, 3156 (1991).
[13]L. Krusin-Elbaum, A. P. Malozemoff, Y. Yeshurun, D. C. Cronemeyer, and F. Holtzberg, Phys. Rev. B **39**, 2936 (1989).
[14]A. A. Abrikosov, Zh. Eksp. Teor. Fiz. **46**, 1464 (1964) [Sov. Phys. JETP **19**, 988 (1964)].
[15]L. Civale, T. K. Worthington, and A. Gupta, Phys. Rev. B **43**, 5425 (1991).
[16]V. B. Geshkenbein, V. M. Vinokur, and R. Fehrenbacher, Phys. Rev. B **43**, 3748 (1991).
[17]A. Shaulov and D. Dorman, Appl. Phys. Lett. **53**, 2680 (1988).
[18]L. Civale, T. K. Worthington, L. Krusin-Elbaum, and F. Holtzberg, *Proceedings of the Workshop on Magnetic Susceptibility of Superconductors* (Plenum, New York, 1992), p. 1234.
[19]J. R. Clem, H. R. Kerchner, and S. T. Sekula, Phys. Rev. B **14**, 1893 (1976).
[20]J. R. Clem and M. W. Coffey, Phys. Rev. B **46**, 14 662 (1992).
[21]T. K. Worthington, F. Holtzberg, and C. A. Feild, Cryogenics **30**, 417 (1990).
[22]C. P. Bean, Phys. Rev. Lett. **8**, 250 (1962).
[23]R. H. Koch, V. Foglietti, W. J. Gallagher, G. Koren, A. Gupta, and M. P. A. Fisher, Phys. Rev. Lett. **63**, 1511 (1989).
[24]P. H. Kes *et al.*, Supercon. Sci. Technol. **1**, 242 (1989).
[25]E. H. Brandt, Z. Phys. B **80**, 167 (1990).
[26]A. M. Campbell, J. Phys. C **2**, 1492 (1969).
[27]U. Welp, W. K. Kwok, G. W. Crabtree, K. G. Vandervoort, and J. Z. Liu, Phys. Rev. Lett. **62**, 1908 (1989).
[28]A. A. Abrikosov, *Fundamentals of the Theory of Metals* (North-Holland, Amsterdam, 1988).
[29]V. G. Kogan, Phys. Rev. B **24**, 1572 (1981).
[30]D. Saint-James and P. G. de Gennes, Phys. Lett. **7**, 306 (1963).
[31]J. Guimpel, L. Civale, F. de la Cruz, J. Murduck, and I. Schuller, Phys. Rev. B **38**, 2342 (1988).
[32]M. Tinkham, *Introduction to Superconductivity* (Krieger, Malabar, 1975).
[33]C. P. Bean and J. D. Livingston, Phys. Rev. Lett. **12**, 14 (1964).
[34]L. Civale and F. de la Cruz, Phys. Rev. B **36**, 3560 (1987).